Virology 379 (2008) 175–180

Contents lists available at ScienceDirect

Virology

journal homepage: www.elsevier.com/locate/yviro

Rapid Communication

Proteolytic processing of polyproteins 1a and 1ab between non-structural proteins 10 and 11/12 of *Coronavirus* infectious bronchitis virus is dispensable for viral replication in cultured cells

Shou Guo Fang [a], Hongyuan Shen [a], Jibin Wang [b], Felicia P.L. Tay [a], Ding Xiang Liu [a,b,*]

[a] *Institute of Molecular and Cell Biology, 61 Biopolis Drive, Proteos, Singapore 138673, Singapore*
[b] *School of Biological Sciences, Nanyang Technological University, 60 Nanyang Drive, Singapore 637551, Singapore*

ARTICLE INFO

Article history:
Received 31 May 2008
Returned to author for revision 13 June 2008
Accepted 28 June 2008
Available online 3 August 2008

Keywords:
Coronavirus
3C-like proteinase
Cleavage sites
nsp10–nsp11/12
Replication

ABSTRACT

Coronavirus 3C-like proteinase (3CLpro) plays important roles in viral life cycle through extensive processing of the polyproteins 1a and 1ab into 12 mature, non-structural proteins (nsp5–nsp16). Structural and biochemical studies have revealed that all confirmed 3CLpro cleavage sites have a conserved Gln residue at the P1 position, which is thought to be absolutely required for efficient cleavage. Recent studies on murine hepatitis virus (MHV) showed that processing of the 1a polyprotein at the position between nsp10–nsp11 is essential for viral replication. In this report, we investigated the requirement of processing at the equivalent position for replication of avian coronavirus infectious bronchitis virus (IBV), using an infectious cloning system. The results showed that mutation of the P1 Gln to Pro or deletion of the Gln residue in the nsp10–nsp11/12 site completely abolished the 3CLpro-mediated processing, but allowed production of infectious recombinant viruses with variable degrees of growth defect, suggesting that cleavage at the nsp10–nsp11/12 site of IBV is dispensable for viral replication in cultured cells. This study would pave a way for potential vaccine development by generation of attenuated IBV from field isolates through manipulation of the nsp10–nsp11/12 cleavage site. Similar approaches would be also applicable to other human and animal coronaviruses.

Introduction

Coronavirus-encoded 3C-like proteinase (3CLpro), also known as main proteinase, plays a pivotal role in viral replication. It mediates cleavage of the replicase polyproteins 1a and 1ab at 11 specific sites, generating 12 mature non-structural proteins (nsp) (from nsp5–16) and, probably, functional intermediates involved in the replication and transcription of viral RNA (Ziebuhr et al., 2000; Ziebuhr, 2005; Masters, 2006). The substrate specificity of coronavirus 3CLpro is determined mainly by the P1, P2 and P1′ positions. Comparative analyses of 77 cleavage sites of 3CLpro from seven coronaviruses suggest amino acid conservation at the P2 (Leu, Val, Ile, Phe, and Met), P1 (Gln) and P1′ (Ser, Ala, Gly, Asn, and Cys) positions. Among them, the P1 position is exclusively occupied by a Gln and the bulky hydrophobic residues (mainly Leu) are dominant at the P2 position (Ziebuhr et al., 2000; Thiel et al., 2003; Gao et al., 2003). Insights into the catalytic activity and substrate specificity of 3CLpros obtained by recent determination of the crystal structure of 3CLpros from coronavirus transmissible gastroenteritis virus (TGEV), human coronavirus 229E (HCoV-229E), severe acute respiratory syndrome coronavirus (SARS-CoV) and infectious bronchitis virus (IBV) confirm the necessity of conservation at the P1 position of the substrates (Anand et al., 2002, 2003; Yang et al., 2003; Xue et al., 2008).

IBV, a member of the group 3 coronavirus, contains a 27.6 kb of genomic RNA. Its replicase gene encodes two large overlapping ORFs (1a and 1b) at the 5′-end of the genome, and translation of the replicase gene yields polyproteins 1a of 441 kDa and 1ab of 741 kDa via a (−1) ribosomal frameshifting (Boursnell et al., 1987; Brierley et al., 1987, 1989). The two polyproteins are processed extensively by virus-encoded papain-like proteinase (PLP) and 3CLpro to produce 15 mature functional products and multiple intermediates associated with viral replication (Gorbalenya et al., 1989; Tibbles et al., 1996; Liu et al., 1994, 1995, 1997, 1998; Liu and Brown, 1995; Ng and Liu, 1998, 2000, 2002; Lim and Liu, 1998; Lim et al., 2000; Xu et al., 2001) (Fig. 1a). Like its homologs in other coronaviruses, the IBV 3CLpro is encoded by ORF1a and resides in nsp5. The proteinase mediates specific cleavage of IBV polyproteins 1a and 1ab at 11 sites to produce 12 mature products (Fig. 1a).

In recent years, the structures and functions of coronavirus nsp are emerging (Bartlam et al., 2007). However, the exact roles and necessity of 3CLpro-mediated processing at individual cleavage sites as well as the functions of specific cleavage intermediates in the life cycle of a given coronavirus are poorly understood. In a recent study, proteolytic processing at the cleavage sites between nsp6–nsp7, nsp7–

* Corresponding author. Institute of Molecular and Cell Biology, 61 Biopolis Drive, Proteos, Singapore 138673, Singapore.
E-mail address: dxliu@imcb.a-star.edu.sg (D.X. Liu).

0042-6822/$ – see front matter © 2008 Elsevier Inc. All rights reserved.
doi:10.1016/j.virol.2008.06.038

nsp8, nsp8–nsp9, and nsp10–nsp11 of murine hepatitis virus (MHV) was shown to be essential for replication of MHV in cultured cells (Deming et al., 2007). In this report, we used an established reverse genetic system to investigate the requirement of processing at the position between nsp10–nsp11/12 for IBV replication. In contrast to the results reported by Deming et al. (2007) for MHV, mutation or deletion of the conserved P1 Gln residue (Gln3928) showed that proteolytic processing of the IBV polyproteins 1a and 1ab at this position is dispensable for virus replication in cultured cells. Mutation of the Gln3928 residue to Pro (Q3928P) or deletion of Gln3928 (ΔQ3928) completely abolished the 3CLpro-mediated processing at the position, but allowed recovery of mutant viruses with no detectable cleavage at the position between nsp10–nsp11/12 in cells infected with the recovered mutant viruses. The mutant viruses showed variable degrees of growth defect, revealing a potential way for generation of attenuated viruses for vaccine development.

Result and discussion

Deletion and mutational analysis of the Q3928–S3929 cleavage site between nsp10 and nsp11/12 of IBV

Introduction of point mutation and deletion into the P1 position of the IBV 3CLpro cleavage site between nsp10 and nsp11/12 was carried out either by replacing the P1 Gln residue with a Pro (Q3928P) and an Asn (Q3928N), respectively, or by deleting the P1-Gln (ΔQ3928) (Fig. 1a). To check the effect of these manipulations on the cleavability of the substrate, IBV sequence (12100–12719 nucleotide) flanking this cleavage site was amplified by RT-PCR, and cloned into a vector in frame with a FLAG tag at the N-terminus (Fig. 1a). To facilitate detection of the cleavage products, an additional T was inserted between nucleotides 12347 and 12348, resulting in the extension of the ORF1a frame to the end of the fragment (nucleotide position 12719) (Fig. 1a). To analyze the 3CLpro-mediated processing, IBV 3CLpro was co-expressed with the mutant constructs in Vero cells using the recombinant vaccinia virus/T7 system. Western blotting analysis with anti-FLAG antibody showed that 3CLpro was able to completely cleave the wild type substrate; a cleavage product with predicted molecular mass of 9.1 kDa was detected (Fig. 1b, lane 2). However, the enzyme failed to process the mutant substrates, as the same cleavage product was not detected in cells co-expressing 3CLpro and the three mutant constructs (Fig. 1b, lanes 3–5).

Introduction of the point mutations (Q3928N and Q3928P) and deletion (ΔQ3928) into the IBV genome and recovery of infectious virus

The Q3928P, Q3928N and ΔQ3928 mutations/deletion were then introduced into the IBV genome using the reverse genetic system

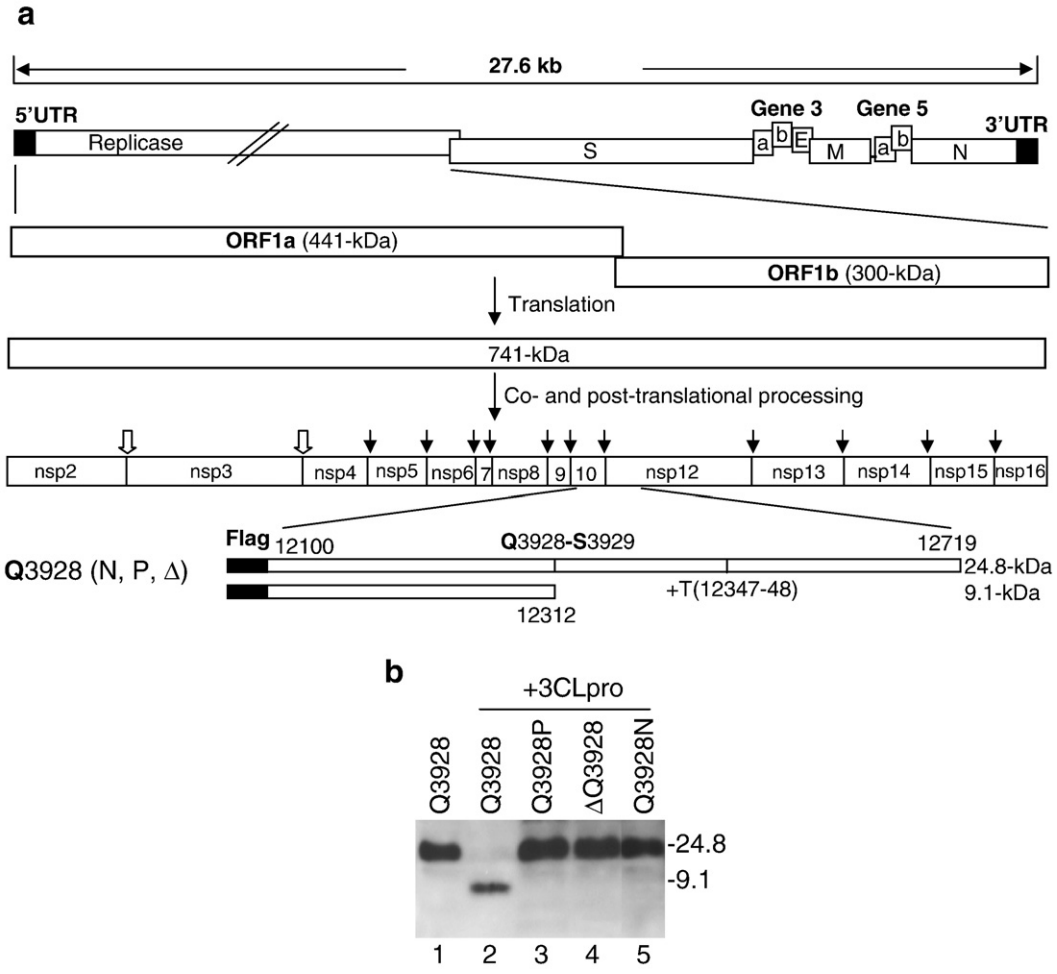

Fig. 1. (a) IBV genome organization and proteolytic processing of IBV replicase polyproteins. Shown are the replicase polyproteins 1a and 1ab of IBV. The processing end-products of 1a are designated non-structural proteins (nsp) 2 to nsp11, and those of polyprotein 1ab are designated nsp2 to nsp10 and nsp12 to nsp16. The cleavage sites of IBV 3CLpro are indicated with black arrow. The cleavage sites of papain-like proteinase (PLP) are indicated with block arrow. (b) Effect of deletion and mutation of the P1 residue at the cleavage site between nsp10–nsp11/12. Plasmids carrying wild type and mutant IBV sequences from nucleotides 12100–12729 with insertion of an extra T at position between nucleotides 12347–12348 were co-expressed with the IBV 3CLpro in Vero cells using the vaccinia virus-T7 system. Cells were harvested at 16 h post-transfection, lysates were prepared and separated on 15% SDS-PAGE. Western blot was performed using anti-FLAG antibody. The cleaved product (9.1 kDa) and uncleaved substrate (24.8 kDa) were indicated.

previously described (Tan et al., 2006; Fang et al., 2007). Full-length transcripts were generated and electroporated into Vero cells. At two days post-electroporation, typical CPE were observed in the cells electroporated with wild type and all mutant transcripts. When the clarified media from the electroporated cells were used to infect fresh Vero cells, CPE was found at 16 h post-infection, confirming the production of infectious progeny viruses.

Characterization of the growth kinetics of the recovered mutant viruses and identification of nsp10–12 chimeric protein in cells infected with the mutant viruses

Growth kinetics of the recovered mutant viruses Q3928P, Q3928N and ΔQ3928 were analyzed by $TCID_{50}$ assay. Compared to wild type rIBV, Q3928P mutant virus displayed very similar growth kinetics as the wild type virus; both viruses reached the peak at 16 h post-infection with peak titer of 10^6 for wild type virus and a slightly lower $TCID_{50}$ for the mutant virus (Fig. 2a). The Q3928N mutant virus reached the peak titer of 10^6 at 12 h post-infection (Fig. 2a). The ΔQ3928 mutant virus displayed approximately 10-fold lower peak $TCID_{50}$ value at 16 h post-infection (Fig. 2a). Interestingly, it was observed that this mutant virus maintained a titer similar to the peak value up to 36 h post-infection (Fig. 2a). All mutant viruses showed similar sized plaques in Vero cells at 4 days post-infection (data not shown).

Radioimmunoprecipitation was then carried out to analyze the processing of nsp10–nsp11/12 in cells infected with the mutant viruses. A predominant cleavage product with an approximately molecular mass of 100 kDa, representing the nsp12 protein, was detected in cells infected with wild type rIBV (Fig. 2b, lane 2). A minor band of approximately 120 kDa was also detected in the same cell lysates (Fig. 2b, lane 2); it may represent the nsp10–nsp12 intermediate cleavage product. In cells infected with the Q3928P and ΔQ3928 mutant viruses, only the 120 kDa species was detected (Fig. 2b, lanes 4 and 5). Unexpectedly, in cells infected with the Q3928N mutant virus, both the 100 kDa and the 120 kDa species were detected, although detection of slightly more 120 kDa species was observed (Fig. 2b, lane 3), suggesting that this mutation did not completely ablate cleavage at this position in cells infected with the mutant virus. Attempts to detect the nsp10–11 intermediate in cells infected with wild type and mutant viruses were unsuccessful, due to the low quality of the available antibodies against nsp10. As a control for the efficiency of IBV infection, cells infected with wild type and the ΔQ3928 mutant virus, respectively, were analyzed by immunoprecipitation analysis with anti-IBV S protein antibodies, showing the presence of glycosylated full-length (S^a), unglycosylated full-length (S^b) species (Fig. 2b, lanes 6–8). The cleaved S1/S2 (S^c) species were also marginally detected in this gel (Fig. 2b, lanes 6–8), and much more clear detection of these species was obtained in longer exposed gels (data not shown). These results confirmed that either mutation of the Q3928 residue to a Pro or deletion of the Q3928 residue totally blocked the IBV 3CLpro-mediated cleavage at the position. However, viable viruses with reasonably good replication efficiency could be recovered from in vitro transcribed full-length RNAs containing the mutation/deletion.

Continuous passage and genetic stability of the mutant viruses in cultured cells

The genetic stability of these mutant viruses was then tested by continuous propagation of the plaque-purified viruses in Vero cells to 20 passages. Total RNA was extracted from cells infected with wild type rIBV and the mutant viruses at a multiplicity of infection of approximately 1 and Northern blot was performed. The results showed that no significant difference in either the pattern of RNA species or the ratio of RNA1 to RNA6 was found in rIBV and mutant viruses (Fig. 3a, lanes 2–5). Nucleotide sequencing analysis of the RT-PCR products amplified from nsp10 through nsp11 confirmed the presence of the engineered mutations or deletion in the mutant viruses (Fig. 3b). No other nucleotide changes were found in this region (data not shown). These results confirmed that the recovered mutant viruses were stable in cultured cells.

The dispensability of cleavage at this position for IBV replication and infectious virus recovery was further tested by creating a mutant virus with deletion of both the P1-Q3928 and the P1′-S3929 residues (ΔQ3928–S3929). Similarly, propagation of the plaque-purified virus for 20 passages showed that this mutant virus was genetically stable in cultured cells but with slightly lower growth efficiency than wild type and other mutant viruses (Fig. 3a, lane 6 and Fig. 3b).

Cleavage of the polyproteins 1a and 1ab at the position between Q3928 and S3929 by the IBV 3CLpro leads to the release of nsp10 (16 kDa), nsp11 (23 amino acids) and nsp12 (100 kDa) (Liu and Brown, 1994, Liu et al., 1997, Ng and Liu, 2002). Nsp12 encodes the putative viral RNA-dependent RNA polymerase, a critical enzyme that directly controls the replication and transcription of viral RNA. Coronavirus nsp10 may function in the formation of viral replication/transcription complexes. It was reported that IBV nsp10 may form dimers and localize to membranes associated with RNA synthesis (Ng and Liu, 2002); and MHV nsp10 colocalizes with nsp1, nsp2, nsp5, nsp7, nsp8, nsp9, nsp12, nsp13 and nucleocapsid protein at the site of replication

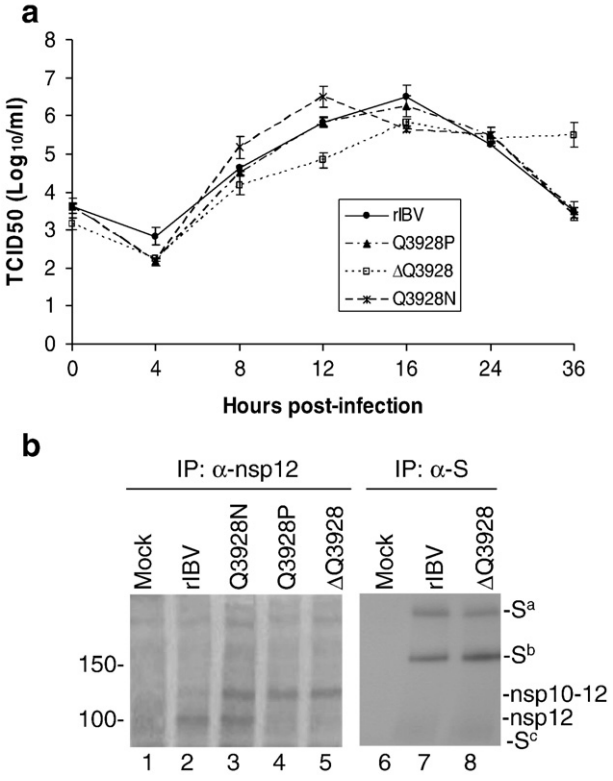

Fig. 2. (a) Analysis of the growth properties of wild type and mutant viruses. Vero cells were infected with wild type (rIBV) and three mutant viruses Q3928N, Q3928P and ΔQ3928 at a multiplicity of infection of approximately 1. Cells were harvested at 0, 4, 8, 12, 16, 24 and 36 h post-infection, respectively. Viral stocks were prepared by freezing/thawing of the cells three times, and $TCID_{50}$ of each viral preparation was determined by infection of five wells of Vero cells on 96-well plates in triplicate with 10-fold serial dilution of each viral stock. (b) Processing of nsp10–nsp12 in wild type and mutant viruses. Vero cells were infected with rIBV, Q3928N, Q3928P and ΔQ3928, respectively, at a multiplicity of infection of approximately 1 for 4 h and labeled with ^{35}S-Met-containing medium for 16 h. Cells were harvested, lysed and proteins were immunoprecipitated with polyclonal antiserum against IBV nsp12. After resolved by 6% SDS-PAGE, proteins were detected by fluorography. Bands corresponding to nsp12 (100 kDa, nsp12) and the nsp10–nsp12 fusion protein (120 kDa, nsp10–12) are indicated.

complexes (Bost et al., 2000; Brockway et al., 2003). More recently, the protein was shown to be involved in the synthesis of MHV RNA (Sawicki et al., 2005), by functioning as a critical regulator of viral RNA synthesis (Donaldson et al., 2007b). It may also play a role in regulation of polyprotein processing (Donaldson et al., 2007a). Structural studies of the SARS-CoV nsp10 showed that it is a novel zinc finger protein with two zinc-binding motifs and 12 identical subunits assemble into a novel functional dodecameric architecture that forms a hollow, positively charged cylinder (Su et al., 2006; Joseph et al., 2006). Based on this information, the protein was proposed to be a transcription factor (Su et al., 2006). In this study, we provided concrete genetic and biochemical evidence that proteolytic processing at the cleavage sites between the two proteins is not required for their functions in viral replication. It suggests that the nsp10–12 intermediate may play the functions of both nsp10 and nsp12 in virus-infected cells. It is puzzling that two such critical functional proteins would retain their individual functionality in the form of a processing intermediate. Interestingly, our results are in sharp contrast to a recently reported result that processing of nsp10–nsp11/12 was essential for MHV replication (Deming et al., 2007). The reason for this remarkable discrepancy is not known. Nevertheless, it demonstrates that different RNA viruses, even among viruses in the same family, may employ totally different strategies to regulate their RNA replication. In addition, our data would indirectly support the proposal that the fused nsp10–nsp11 could be crystallized into a novel functional dodecameric architecture (Su et al., 2006).

Mutational analysis and peptide cleavage data have shown that replacement of the conserved P2 Leu residue with a Val could significantly decrease the cleavage efficiency in several positions (Fan et al., 2004, 2005). The nsp10–nsp11/12 site of IBV has a Val instead of Leu residue at the P2 position and the P2 positions of nsp10–nsp11/12 in other coronaviruses are also occupied by noncanonical residues (Ziebuhr and Siddell, 1999, Fan et al., 2004). In this study, a minute amount of the nsp10–nsp12 intermediate was detected in cells infected with wild type IBV. This intermediate cleavage product would therefore maintain the functions of both nsp10 and nsp12 proteins, making it more difficult to design peptide inhibitors. On the other hand, it is reasonable to speculate that the full functions of the two proteins may depend on one another. For example, it is not yet confirmed that nsp12 is the coronavirus RNA-dependent RNA polymerase due to the lack of concrete biochemical data. One possibility is that inclusion of nsp10 in the in vitro experiment system would be needed in order to detect the full function of nsp12, especially the activity involved in de novo synthesis of the full-length coronavirus RNA using purified nsp12. The fact that minute amounts of the nsp10–12 intermediate were detected in cells infected with wild type IBV further supports that the two proteins may function synergistically.

As the recovered mutant viruses showed certain degrees of growth defect, one potential application of this study is to create attenuated viruses by deletion of the Q3928–S3929 site and the flanking sequences for development of vaccine candidates. For example, infectious virus recovered from construct with deletion of the Q3928 residue is stable and showed slow growth kinetics with lower peak titer. Furthermore, infectious virus with even lower replication efficiency could also be recovered from construct with deletion of both Q3928–S3929 residues. Manipulation of this position would create attenuated viruses suitable for development of IBV vaccines from new isolates. Meanwhile, manipulation of the same position in other human and animal coronaviruses, such as SARS-CoV, might be able to create attenuated viruses for the same purpose. Further insights into the practicality of this approach in vaccine development would be provided by systematic studies to confirm if mutant viruses generated by this manipulation were also attenuated in pathogenesis as well as the stability and recombination rate of the mutant viruses in animals.

Materials and methods

Cells and virus

Vero cells were cultured at 37 °C in minimal essential medium (MEM) supplemented with 10% fetal bovine serum (FBS), penicillin (100 units/ml), and streptomycin (100 μg/ml). Recombinant wild type IBV (rIBV) and mutant IBV were propagated in Vero cells in FBS-free MEM.

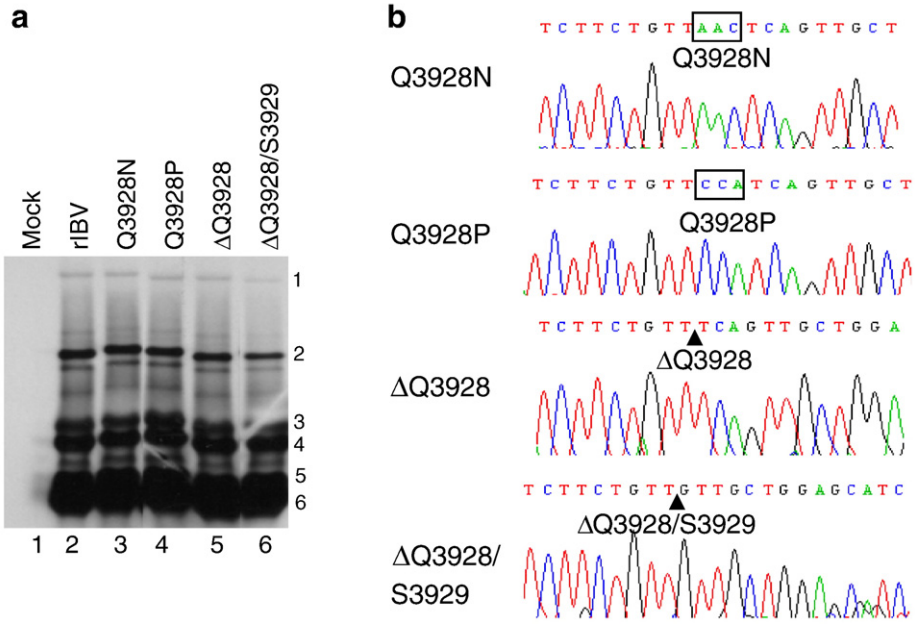

Fig. 3. (a) Northern blot analysis of RNA synthesis in cells infected with wild type IBV and passage 20 of the mutant viruses Q3928N, Q3928P and ΔQ3928, respectively. Vero cells were infected with wild type and the mutant viruses at a multiplicity of infection of approximately 1, and harvested at 16 h post-infection. Total RNA was extracted from the infected cells and separated on a 0.8% denatured agarose gel. After transferring to nylon membrane, viral RNAs were detected by hybridization with a DIG-labeled DNA probe specific for the 3′-UTR of IBV. (b) Genetic stability of the mutant viruses. Total RNA was prepared from Vero cells infected with passage 20 of the mutant virus Q3928N, Q3928P, ΔQ3928 and ΔQ3928–S3929, and the region covering mutation or deletion was amplified by RT-PCR and sequenced. The changed or deleted nucleotides were indicated.

Transient expression and processing in mammalian cells

ORFs placed under the control of a T7 promoter were expressed transiently in mammalian cells using a vaccinia-T7 expression system. Briefly, confluent Vero cells in 6-well plate were inoculated with a recombinant vaccinia virus (vTF7-3) expressing T7 RNA polymerase. At 1 h post-infection, medium was removed and plasmids, containing wild type or mutated cleavage site between nsp10–nsp11/12 together with pIBV3C containing the full-length IBV 3CLpro sequence (Liu et al., 1997), were transfected into cells with Lipofectamine 2000 transfection reagent according to the manufacturer's instructions (Invitrogen). Cells were harvested after incubation at 37 °C for 16–20 h.

SDS-PAGE and Western blot analysis

Transfected cells were lysed with 2 × SDS loading buffer containing 100 mM DTT and 5 mM of iodoacetamide, boiled at 100 °C for 5 min and clarified. The proteins were separated by 15% SDS-PAGE and were transferred to PVDF membrane (Bio-Rad). The membrane was blocked overnight at 4 °C or for 2 h at room temperature in blocking buffer (10% fat free milk powder in PBS buffer containing 0.1% Tween-20), and then was incubated with 1:1000 diluted anti-FLAG HRP (Sigma) in blocking buffer for 2 h at room temperature. After washing three times with PBST, the polypeptides were detected with a chemiluminescence detection kit (ECL, Amersham Biosciences) according to the manufacturer's instructions.

Generation of mutant viruses

Constructs containing a single mutation of Gln3928 to Asn or Pro, a deletion of Gln3928 or Gln3928–S3929 were produced by using QuickChange site-directed mutagenesis kit (Stratagene). The mutations were verified by automated nucleotide sequencing.

The full-length infectious clone was assembled as previously described (Tan et al., 2006; Fang et al., 2007) by replacing the corresponding fragment with the mutant fragment. In vitro full-length transcripts were generated using the mMessage mMachine T7 kit (Ambion, Austin, TX) and electroporated into Vero cells with one pulse at 450 V, 50 μF with a Bio-Rad Gene Pulser II electroporator. The electroporated Vero cells were cultured overnight in 1% FBS-containing MEM and further cultured in MEM without FBS. The transfected cells were monitored daily for formation of cytopathic effect (CPE), and the recovered mutant viruses were plaque-purified and propagated in Vero cells.

Northern hybridization

Vero cells were infected with wild type rIBV and the recovered mutant viruses at a multiplicity of ~1 PFU/cell, respectively, and 10 μg of total RNA extracted from the infected cells was added to a mixture of 1 × MOPS, 37% formaldehyde and formamide, and incubated at 65 °C for 20 min prior to gel electrophoresis. The separated RNA bands were transferred onto a Hybond N+ membrane (Amersham Biosciences) via capillary action overnight and fixed by ultraviolet crosslinking (Stratalinker). Hybridization of Dig-labeled DNA probes corresponding to the IBV 3′-untranslated region from nucleotides 27104–27510 was carried out at 50 °C in hybridization buffer oven overnight. Membranes were washed three times for 15 min each with buffers of different stringencies and signals were detected with CDPStar (Roche) according to the manufacturer's instructions.

Viral growth assays

Confluent monolayer of Vero cells on six-well plates was infected with recovered viruses and harvested at different times post-infection. Viral stocks were prepared by freezing/thawing of the cells three times. The 50% tissue culture infection dose ($TCID_{50}$) of each sample was determined by infecting five wells of Vero cells on 96-well plates with 10-fold serial dilution of each viral stock.

Immunoprecipitation analysis

Vero cells were infected with wild type and the mutant viruses. At 2 h post-infection, the cultured media were replaced with methionine-free media. After incubation for 2 h, cells were labeled with ^{35}S-methionine for 16 h. The labeled cells were lysed with 1 ml of RIPA buffer (50 mM Tris–HCl, pH 7.5, 150 mM NaCl, 1% NP-40, 1% sodium deoxycholate, and 0.1% SDS), and immunoprecipitation was performed as described previously using polyclonal antibodies against IBV S and nsp12 proteins (Liu et al., 1994).

Acknowledgment

This work was supported by the Agency for Science, Technology and Research, Singapore.

References

Anand, K., Palm, G.J., Mesters, J.R., Siddell, S.G., Ziebuhr, J., Hilgenfeld, R., 2002. Structure of coronavirus main proteinase reveals combination of a chymotrypsin fold with an extra alpha-helical domain. EMBO J. 21, 3213–3224.

Anand, K., Ziebuhr, J., Wadhwani, P., Mesters, J.R., Hilgenfeld, R., 2003. Coronavirus main proteinase (3CLpro) structure: basis for design of anti-SARS drugs. Science 300, 1763–1767.

Bartlam, M., Xu, Y., Rao, Z., 2007. Structural proteomics of the SARS coronavirus: a model response to emerging infectious diseases. J. Struct. Funct. Genomics 8, 85–97.

Bost, A.G., Carnahan, R.H., Lu, X.T., Denison, M.R., 2000. Four proteins processed from the replicase gene polyprotein of mouse hepatitis virus colocalize in the cell periphery and adjacent to sites of virion assembly. J. Virol. 74, 3379–3387.

Boursnell, M.E.G., Brown, T.D.K., Foulds, I.J., Green, P.F., Tomely, F.M., Binns, M.M., 1987. Completion of the sequence of the genome of the coronavirus avian infectious bronchitis virus. J. Gen. Virol. 68, 57–77.

Brierley, I., Boursnell, M.E.G., Binns, M.M., Bilimoria, B., Blok, V.C., Brown, T.D.K., Inglis, S.C., 1987. An efficient ribosomal frame-shifting signal in the polymerase-encoding region of the coronavirus IBV. EMBO J. 6, 3779–3785.

Brierley, I., Digard, P., Inglis, S.C., 1989. Characterization of an efficient coronavirus ribosomal frameshifting signal: requirement for an RNA pseudoknot. Cell 57, 537–547.

Brockway, S.M., Clay, C.T., Lu, X.T., Denison, M.R., 2003. Characterization of the expression, intracellular localization, and replication complex association of the putative mouse hepatitis virus RNA-dependent RNA polymerase. J. Virol. 77, 10515–10527.

Deming, D.J., Graham, R.L., Denison, M.R., Baric, R.S., 2007. Processing of open reading frame 1a replicase proteins nsp7 to nsp10 in murine hepatitis virus strain A59 replication. J. Virol. 81, 10280–10291.

Donaldson, E.F., Graham, R.L., Sims, A.C., Denison, M.R., Baric, R.S., 2007a. Analysis of murine hepatitis virus strain A59 temperature-sensitive mutant TS-LA6 suggests that nsp10 plays a critical role in polyprotein processing. J. Virol. 81, 7086–7098.

Donaldson, E.F., Sims, A.C., Graham, R.L., Denison, M.R., Baric, R.S., 2007b. Murine hepatitis virus replicase protein nsp10 is a critical regulator of viral RNA synthesis. J. Virol. 81, 6356–6368.

Fan, K., Ma, L., Han, X., Liang, H., Wei, P., Liu, Y., Lai, L., 2005. The substrate specificity of SARS coronavirus 3C-like proteinase. Biochem. Biophys. Res. Commun. 329, 934–940.

Fan, K., Wei, P., Feng, Q., Chen, S., Huang, C., Ma, L., Lai, B., Pei, J., Liu, Y., Chen, J., Lai, L., 2004. Biosynthesis, purification, and substrate specificity of severe acute respiratory syndrome coronavirus 3C-like proteinase. J. Biol. Chem. 279, 1637–1642.

Fang, S.G., Chen, B., Tay, F.P.L., Liu, D.X., 2007. An arginine-to-proline mutation in a domain with undefined function within the RNA helicase protein (NSP13) is lethal to the coronavirus infectious bronchitis virus in cultured cells. Virology 358, 136–147.

Gao, F., Ou, H.Y., Chen, L.L., Zheng, W.X., Zhang, C.T., 2003. Prediction of proteinase cleavage sites in polyproteins of coronaviruses and its applications in analyzing SARS-CoV genomes. FEBS Lett. 553, 451–456.

Gorbalenya, A.E., Koonin, E.V., Donchenko, A.P., Blinov, V.M., 1989. Coronavirus genome: prediction of putative functional domains in the non-structural polyprotein by comparative amino acid sequence analysis. Nucleic Acids Res. 17, 4847–4861.

Joseph, J.S., Saikatendu, K.S., Subramanian, V., Neuman, B.W., Brooun, A., Griffith, M., Moy, K., Yadav, M.K., Velasquez, J., Buchmeier, M.J., Stevens, R.C., Kuhn, P., 2006. Crystal structure of nonstructural protein 10 from the SARS coronavirus reveals a novel fold with two zinc-binding motifs. J. Virol. 80, 7894–7901.

Lim, K.P., Liu, D.X., 1998. Characterization of the two overlapping papain-like proteinase domains encoded in gene 1 of the coronavirus infectious bronchitis virus and

determination of the C-terminal cleavage site of an 87 kDa protein. Virology 245, 303–312.
Lim, K.P., Ng, L.F.P., Liu, D.X., 2000. Identification of a novel cleavage activity of the first papain-like proteinase domain encoded by ORF 1a of the coronavirus avian infectious bronchitis virus and characterization of the cleavage products. J. Virol. 74, 1674–1685.
Liu, D.X., Brown, T.D.K., 1995. Characterisation and mutational analysis of an ORF 1a-encoding proteinase domain responsible for proteolytic processing of the infectious bronchitis virus 1a/1b polyprotein. Virology 209, 420–427.
Liu, D.X., Brierley, I., Tibbles, K.W., Brown, T.D.K., 1994. A 100-kilodalton polypeptide encoded by open reading frame (ORF) 1b of the coronavirus infectious bronchitis virus is processed by ORF 1a products. J. Virol. 68, 5772–5780.
Liu, D.X., Shen, S., Xu, H.Y., Wang, S.F., 1998. Proteolytic mapping of the coronavirus infectious bronchitis virus 1b polyprotein: evidence for the presence of four cleavage sites of the 3C-like proteinase and identification of two novel cleavage products. Virology 246, 288–297.
Liu, D.X., Tibbles, K.W., Cavanagh, D., Brown, T.D.K., Brierley, I., 1995. Identification, expression, and processing of an 87-kDa polypeptide encoded by ORF 1a of the coronavirus infectious bronchitis virus. Virology 208, 48–57.
Liu, D.X., Xu, H.Y., Brown, T.D.K., 1997. Proteolytic processing of the coronavirus infectious bronchitis virus 1a polyprotein: identification of a 10 kDa polypeptide and determination of its cleavage sites. J. Virol. 71, 1814–1820.
Masters, P.S., 2006. The molecular biology of coronaviruses. Adv. Virus Res. 66, 193–292.
Ng, L.F., Liu, D.X., 2000. Further characterization of the coronavirus infectious bronchitis virus 3C-like proteinase and determination of a new cleavage site. Virology 272, 27–39.
Ng, L.F., Liu, D.X., 2002. Membrane association and dimerization of a cysteine-rich, 16-kilodalton polypeptide released from the C-terminal region of the coronavirus infectious bronchitis virus 1a polyprotein. J. Virol. 76, 6257–6267.
Ng, L.F.P., Liu, D.X., 1998. Identification of a 24 kDa polypeptide processed from the coronavirus infectious bronchitis virus 1a polyprotein by the 3C-like proteinase and determination of its cleavage sites. Virology 243, 388–395.
Sawicki, S.G., Sawicki, D.L., Younker, D., Meyer, Y., Thiel, V., Stokes, H., Siddell, S.G., 2005. Functional and genetic analysis of coronavirus replicase-transcriptase proteins. PLoS Pathog. 1, e39.
Su, D., Lou, Z., Sun, F., Zhai, Y., Yang, H., Zhang, R., Joachimiak, A., Zhang, X.C., Bartlam, M., Rao, Z., 2006. Dodecameric structure of severe acute respiratory syndrome coronavirus nonstructural protein nsp10. J. Virol. 80, 7902–7908.
Tan, Y.W., Fang, S.G., Fan, H., Lescar, J., Liu, D.X., 2006. Amino acid residues critical for RNA-binding in the N-terminal domain of the nucleocapsid protein are essential determinants for the replication and infectivity of coronavirus in cultured cells. Nucleic Acids Res. 34, 4816–4825.
Thiel, V., Ivanov, K.A., Putics, A., Hertzig, T., Schelle, B., Bayer, S., Weissbrich, B., Snijder, E.J., Rabenau, H., Doerr, H.W., Gorbalenya, A.E., Ziebuhr, J., 2003. Mechanisms and enzymes involved in SARS coronavirus genome expression. J. Gen. Virol. 84, 2305–2315.
Tibbles, K.W., Brierley, I., Cavanagh, D., Brown, T.D.K., 1996. Characterization in vitro of an autocatalytic processing activity associated with the predicted 3C-like proteinase domain of the coronavirus avian infectious bronchitis virus. J. Virol. 70, 1923–1930.
Xu, H.Y., Lim, K.P., Shen, S., Liu, D.X., 2001. Further identification and characterization of novel intermediate and mature cleavage products released from the ORF 1b region of the avian coronavirus infectious bronchitis virus 1a/1b polyprotein. Virology 288, 212–222.
Xue, X., Yu, H., Yang, H., Xue, F., Wu, Z., Shen, W., Li, J., Zhou, Z., Ding, Y., Zhao, Q., Zhang, X.C., Liao, M., Bartlam, M., Rao, Z., 2008. Structures of two coronavirus main proteases: implications for substrate binding and antiviral drug design. J. Virol. 82, 2515–2527.
Yang, H., Yang, M., Ding, Y., Liu, Y., Lou, Z., Zhou, Z., Sun, L., Mo, L., Ye, S., Pang, H., Gao, G.F., Anand, K., Bartlam, M., Hilgenfeld, R., Rao, Z., 2003. The crystal structures of severe acute respiratory syndrome virus main protease and its complex with an inhibitor. Proc. Natl. Acad. Sci. U.S.A. 100, 13190–13195.
Ziebuhr, J., 2005. The coronavirus replicase. Curr. Top. Microbiol. Immunol. 287, 57–94.
Ziebuhr, J., Siddell, S.G., 1999. Processing of the human coronavirus 229E replicase polyproteins by the virus-encoded 3C-like proteinase: identification of proteolytic products and cleavage sites common to pp1a and pp1ab. J. Virol. 73, 177–185.
Ziebuhr, J., Snijder, E.J., Gorbalenya, A.E., 2000. Virus-encoded proteinases and proteolytic processing in the Nidovirales. J. Gen. Virol. 81, 853–879.